OVERSHOOTING TOPS – CHARACTERISTICS AND PROPERTIES

Michaela Valachová[1,2], Martin Setvák[2], Jindřich Šťástka[1,2]

[1] Charles University in Prague, Faculty of Mathematics and Physics, Department of Meteorology and Environment Protection, V Holešovičkách 2, Prague, Czech Republic
[2] Czech Hydrometeorological Institute, Satellite Dept., Na Šabatce 2050/17, Prague, Czech Republic

Abstract

Overshooting tops atop convective storms directly manifest the strength of updrafts which form them and provide us with essential information about the storm from the satellite perspective. These observations can be used to infer information about the storm intensity, possible severity or internal structure. This study focuses on multispectral and temporal characteristics of overshooting tops and their relationship with other storm-top features. The main properties such as structure, composition or appearance in brightness temperature field are summarized and several recent interesting cases are shown. Tops of deep convective clouds are observed from Suomi NPP (VIIRS) and Aqua (MODIS), CALIPSO (CALIOP, WFC) and CloudSat (CPR) satellites from the A-Train. This satellite constellation offers a unique opportunity to study details of storm tops from various instruments flown aboard satellites with very close orbits. The combination of A-train and MSG Rapid Scan observations (5 or 2.5 minute) enables to study both detailed structures and dynamics of storms and leads to better understanding of cloud-top processes and related phenomena.

INTRODUCTION

Overshooting tops (OT) are a clear indicator of strong updrafts within a convective cell and since their early observations they have been associated with severe weather conditions on the Earth´s surface. The OT detections and severe weather relationship over Europe are studied for instance in Bedka (2011), where strong connections with large hail and severe wind events were shown. All the other significant cloud-top features of convective storms are related to the activity of OTs – warm spots and cold-U or cold-ring features in the brightness temperature field, plumes of ice material above the cloud top and jumping cirrus, gravity waves, microphysical processes and transport of water vapour into the lower stratosphere.

From the satellite perspective typical OTs are manifested in an infrared (IR) imagery by very cold pixels and steep brightness temperature (BT) gradients around these, which are the basis of their automated detection methods (e.g. Bedka et al., 2010). In the high-resolution visible (HRV) imagery, OTs can be revealed by their typical "bubble-like" structure and shadows they cast. In "microphysical spectral bands" (at 1.6 - 4.0 µm) they may differ from their surroundings by their cloud-top reflectivity, depending on the particle size and the cloud phase, see e.g. Scorer (1986) or Setvák and Doswell (1991). Moreover, some of the OTs may be associated with higher brightness temperature differences (BTD) between a water vapour (WV) absorption band and an IR-window band above convective storm tops (e.g. Bedka et al., 2010, Setvák et al., 2013). All these properties are discussed, divided into following three chapters and shown on brief case studies. This contribution particularly links up to the first studies using A-train observations by Setvák et al. (2013).

One of the problems related to OTs is that there is no formal threshold for classifying an object as an OT as regards its size (horizontal, vertical) or brightness temperature. With improving satellite image resolution it becomes difficult to determine what structure to consider as an OT and what is just a manifestation of a cloud-top turbulence. The pixel size (spatial resolution) of an instrument determines the size of storm-top features we can discriminate. The better the resolution, the finer details can be resolved and the less averaging occurs (Setvák and Levizzani, 1992).

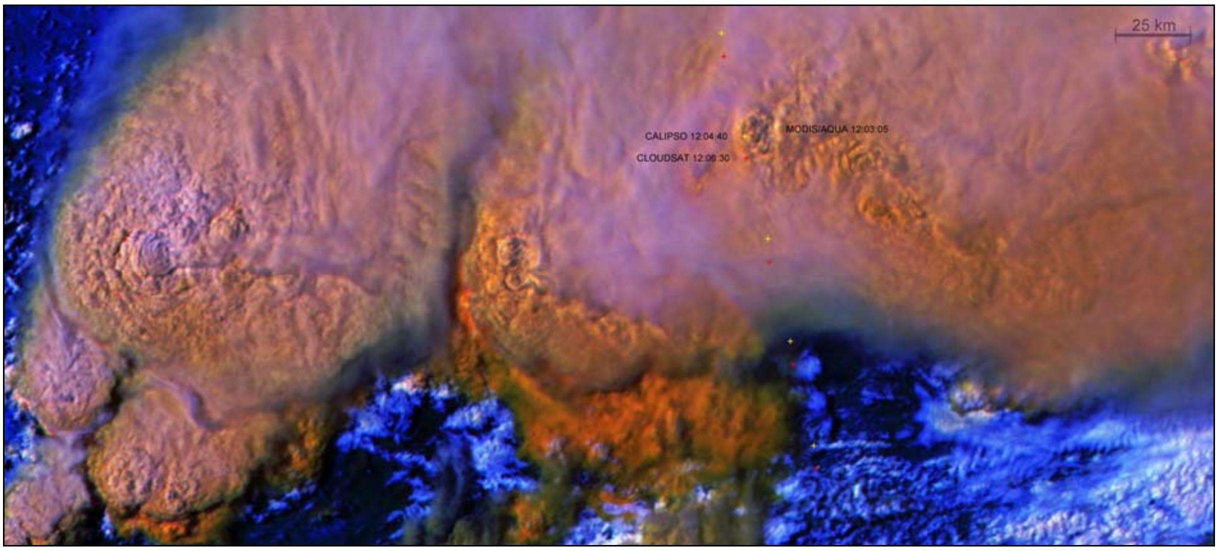

Figure 1: **2012/11/08, 12:03 UTC, MODIS/Aqua. Convective storms above South Africa, RGB product of bands 1 (0.7 µm), 5 (1.2 µm) and 7 (2.1 µm). Crosses indicate ground locations of CloudSat/CPR (red) and CALIPSO/CALIOP (yellow) scan tracks at 5-sec intervals (based on LAT/LON information from HDF data, without a parallax correction).**

METHODOLOGY

Given the fact that the typical size of OTs is of the order of several kilometres across, data from polar orbiting satellites in the high pixel resolution enable finer, more detailed studies of their various properties. Measurements from Suomi NPP satellite were used when available, because observations of VIIRS (Visible Infrared Imaging Radiometer Suite) instrument with the spatial resolution of image bands 371×387 m at nadir and 800×789 m at the swath sides can provide detailed information unreachable ever before.

The vertical structure of convective clouds was examined by combining data from the CloudSat and CALIPSO satellites, which fly in a tight formation. Besides the Cloud Profiling Radar (CPR) and the lidar instrument (Cloud-Aerosol Lidar with Orthogonal Polarization, CALIOP), also the 125-m resolution images from Wide Field Camera (WFC) with a single spectral channel covering the 620-670 nm region were used. The measurements from MODIS (Moderate-Resolution Imaging Spectroradiometer) onboard the Aqua satellite and the geostationary Meteosat satellite rapid scan (2.5 or 5-minute) observations by SEVIRI (Spinning Enhanced Visible and Infrared Imager) were also used, providing information about surroundings and development of the studied storms and their cloud-top features. Source HDF data were visualized using the ENVI, CCPLOT (Kuma, 2010) and Adobe Photoshop CS5 software. Meteosat data (not shown in this paper) from EUMETSAT were provided by Czech Hydrometeorological Institute and displayed by 2met! VISION+.

IR-WINDOW BRIGHTNESS TEMPERATURE

The coldest pixels in IR imagery are typically collocated with a summit of the OT in visible (VIS) images. However, in some cases it is possible to observe distinct BT minima with no matching feature in VIS (HRV) band resembling an OT and vice versa, some of the OTs appear warm, from the very beginning of their occurrence, being detected in VIS bands only (e.g. Setvák et al., 2012). In fact, cold OTs can be detected in IR during their rapid ascent only, not much is known about the rate of OT warming during their descent or collapse. The link between the maturity of the storm and IR BT is shown e.g. in (Luo et al., 2008).

Majority of the observed warm OTs most likely represent OTs in their decaying stage, thus already warming up due to their descent and mixing with surrounding warmer lower stratospheric air. Their BT strongly depends on timing of satellite sampling. Other explanations for warmer OT temperatures can be in lower spatial resolution of the imager aboard some of the satellites, see Setvák and Levizzani

(1992). All this may result in lower detection efficiency of OT using BT-based detection methods (e.g. Dworak et al., 2012 or Bedka et al., 2010). Blending the images in VIS and IR-BT together into sandwich products enables to study OT characteristics and properties in one single image or loops of these, thus observe their evolution (Setvák et al., 2012).

Another storm-top features observed in the IR imagery are cold-U and cold-ring signatures and the embedded warm areas within these features. The formation of these characteristics can be explained (among several other possible explanations) by an interaction of the OT with the upper-level winds. The OT blocks the flow and forces it to divert around it (Wang, 2007). Several hypotheses have been proposed to explain the warm region of BTs, clearly summarized in Brunner et al. (2007) and simulated by a Lagrangian model in Adler and Mack (1986). Cold-U and cold-ring features are well correlated with severe weather (Adler et al., 1985) and were suggested as a possible application of this link for severe weather warnings as far back as in the 1980´s by McCann (1983).

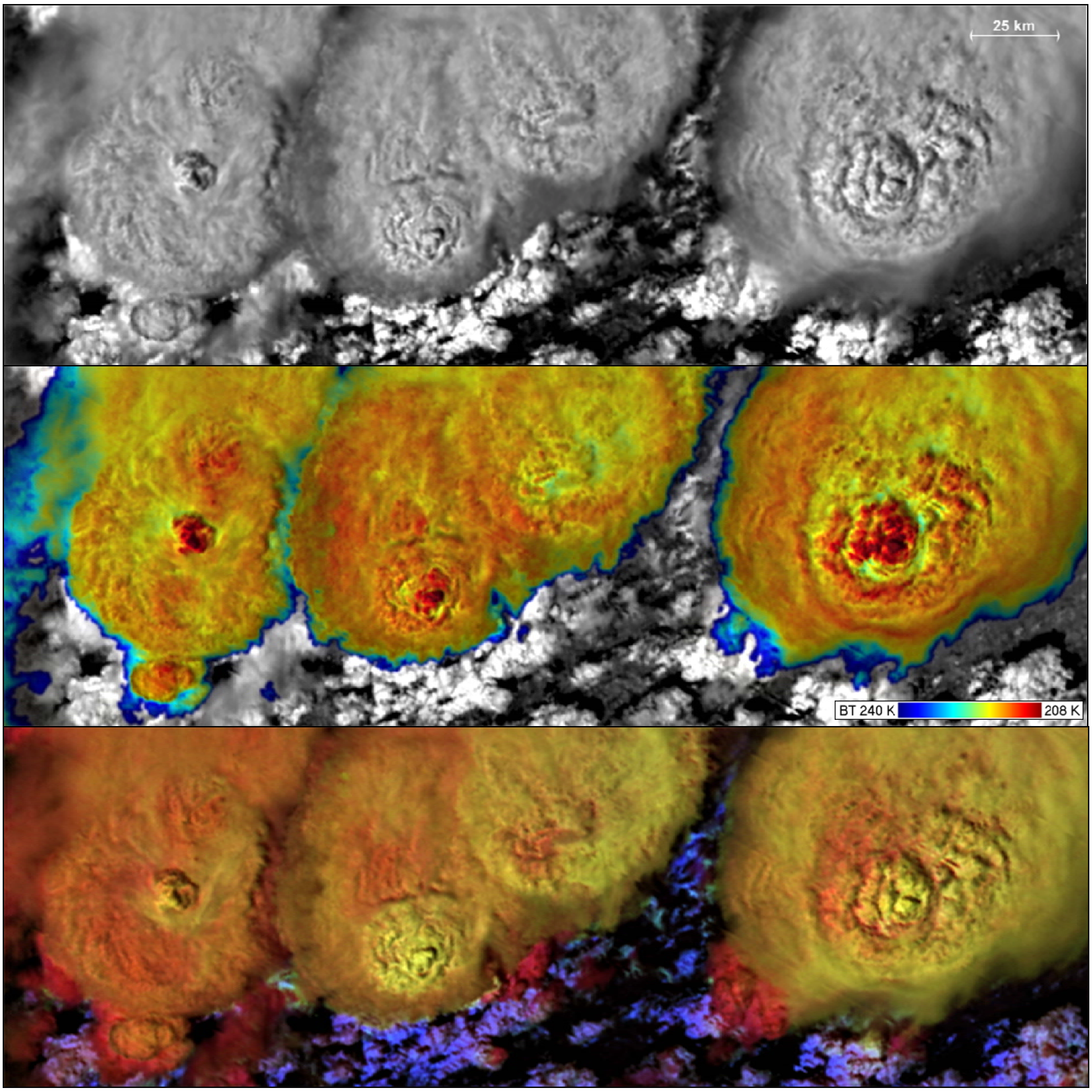

Figure 2: **2012/07/05 12:07 UTC VIIRS/Suomi NPP. Storms over Saxony, east Germany: (top) band I2 (0.9 µm) image, (middle) sandwich product of band I2 and band I5 (11.5 µm) with colour enhanced brightness temperature (208-240 K), (bottom) sandwich RGB product of band I5 in red, brightness temperature difference of band I4 (3.7 µm) and band I5 in green and band I3 (1.6 µm) in blue.**

CLOUD TOP MICROPHYSICS

Many radiative properties closely linked to cloud-top microphysics are connected to bands, which are located in the near-IR range (Scorer 1986). The cloud-top appearance in these bands exhibits a complex dependence on several parameters for both the thermal (temperature, emissivity, transparency) and reflected (reflectivity, transparency, solar zenith angle, geometrical parameters affecting backscattering) components (Levizzani and Setvák, 1996). An increased radiance in channel 3 (3.55 – 3.93 μm) of the AVHRR instrument on tops of some convective storms was first reported by Liljas (1984) and Scorer (1986), pointing out the possibility of the recognition of heterogeneities in their microphysical composition. Setvák and Doswell (1991) reported observations of deep convective storms based on AVHRR´s channels 2 (0.725–1.1 μm), 3 and 4 (10.3–11.3 μm). They show that plume-like features are primarily observed in channel 3 imagery, however, it is possible to resolve them simultaneously or detect them only in VIS channel 1 (0.58 – 0.68 μm) or near-IR channel 2. Levizzani and Setvák (1996) deduced that the observed increased channel 3 reflectivity throughout an entire above-anvil ice plume indicates that source of the ice particles forming the plume has to be persistent without major changes for a longer time.

In strong updrafts small water droplets forming in the cloud base reach the cloud top quickly, have less time to collide and merge to become bigger. Because of homogenous freezing of cloud drops at higher levels small ice particles are produced (Setvák and Doswell, 1991; Rosenfeld et al., 2006). Due to this mechanism, the presence of small ice particles on the storm top can indicate severe updrafts. The reflectivity in „microphysical“ bands (1.6 – 4 μm) is sensitive not only to the cloud phase but also to the cloud particle size (Setvák and Doswell, 1991).

Detailed information about the composition of storm tops can be obtained from CloudSat and CALIPSO measurements. The CloudSat carries the 94-GHz radar measuring power backscattered by cloud droplets or other hydrometeors, whereas CALIPSO includes a dual-wavelength backscattering (polarization-sensitive) lidar instrument, which observes properties of aerosols and μm-sized cloud particles (Kuma, 2010). Additional datasets from passive infrared and visible imagers (IIR, WFC) from CALIPSO were used to better interpret the backscattered signal. These two satellites fly in formation with the Aqua satellite, the radar and lidar footprints should fall in the central part of the MODIS swath.

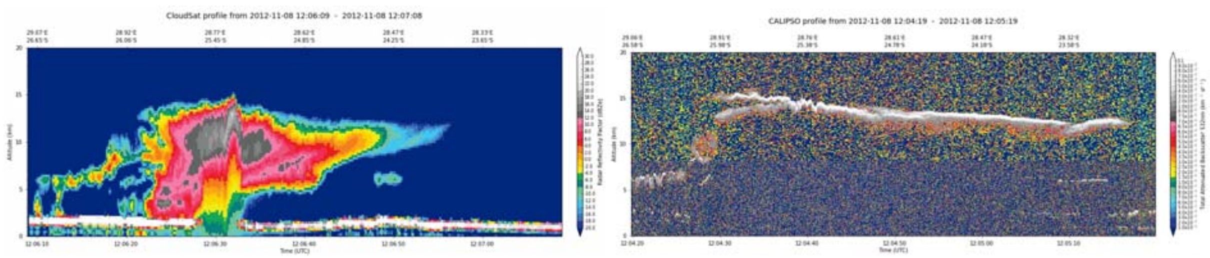

Figure 3: **2012/11/08 Profiles of the storm top along the crosses indicated in Figure 1. CloudSat/CPR reflectivity on the right, CALIPSO/CALIOP Total Attenuated Backscatter at 532 nm profile on the left.**

CLOUD TOP STRUCTURE

To document the detailed vertical structure of the OTs as well as their link to other features on storm tops, the A-train data were used. Although the Aqua satellite flies in close formation with the CloudSat, being separated by only ~2 minutes on nearly collocated tracks, it can be problematic when comparing OT observations from these two instruments. An individual OT may persist for less than 5 minutes, the rapid scan imagery (either the 1-min data from the GOES satellites, or the MSG 2.5-min experimental rapid scan data) shows the high temporal variability of many storm-top features. Thus, it is possible that the MODIS data can show an OT that had either grown or decayed by the time of the CloudSat observation and it should be considered in studies utilizing these datasets.

Moreover, the A-Train measurements do not present the whole history of the convective system that produces OTs. To obtain information about the evolution of convective storms we need observations from geostationary satellites throughout their whole lifecycle. Unfortunately, there is another limitation to the study of convective storms by A-Train measurements – the approximate 1:30 PM equatorial crossing time of the A-Train constellation means that important phases of the diurnal cycle of a deep convection are not sampled.

CASES

5. 7. 2012 Germany

The comparison of the VIS image and the sandwich product in Figure 2 shows OTs in various stages of their evolution. The OTs differ from each other in size and temperatures. The appearance of storm tops varies in the reflectivity in 1.6 µm as well. Higher cloud-top reflectivity represented by yellow tint corresponds to small ice particles, while amber colours indicate the presence of larger ice particles. According to MSG Rapid Scan data (not shown), on the bottom centre there is the youngest storm cell developing within the anvil of an older decaying storm (on the top centre). However, the yellow brightness in the RGB product (Figure 2, bottom) depends also on the IR BT (band I5), contained in the green component. This effect is evident on the OT of the storm on the left, see also the middle part of the figure. For a detailed view of the cloud top structure of the storm on the right see Figure 4.

8. 11. 2012 South Africa

This case of storms exhibiting plume-like features (Figure 1) shows how A-Train data can contribute to a better understanding of phenomena on the storm top. The CALIPSO profile in Figure 3 shows a thin plume at the height of 15 km, vertically separated from the rest of the anvil top by about 1 km. OTs just on the left of the picture centre are probably the source of these ice particles carried downwind to the east. There is no link between this plume and the OT observed by CloudSat and CALIPSO (Figure 1 and 3). According to the CloudSat data this OT is only about 1 km higher than surrounding anvil.

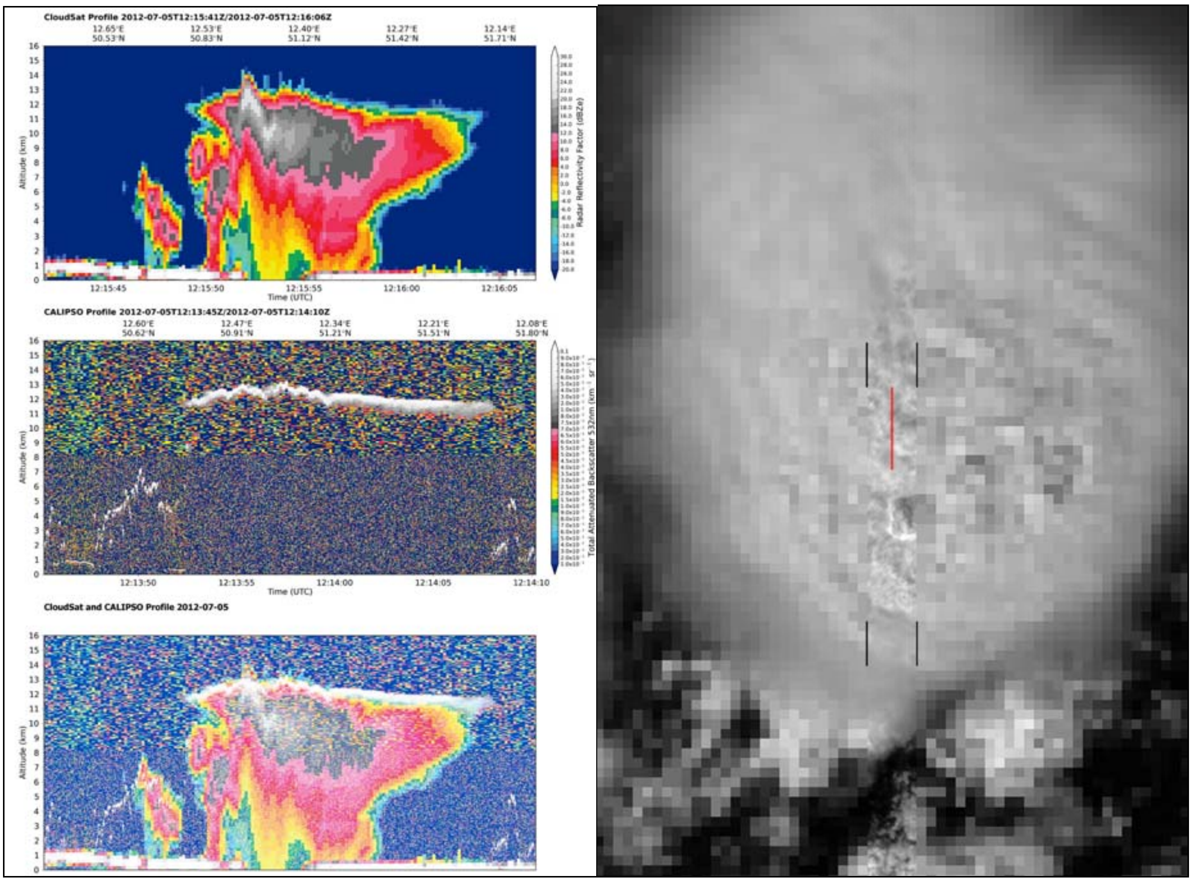

Figure 4: **2012/07/05 Profiles of the storm on the right in Figure 2. (Top left) CloudSat/CPR reflectivity, (middle left) CALIPSO/CALIOP Total Attenuated Backscatter at 532 nm, (bottom left) the overlap of these profiles. (Right) WFC of CALIPSO, consists of 1 km data (outer parts of the swath) and 125 m data (narrow insert in the centre of the swath, indicated by black lines, the centre shown by the red line).**

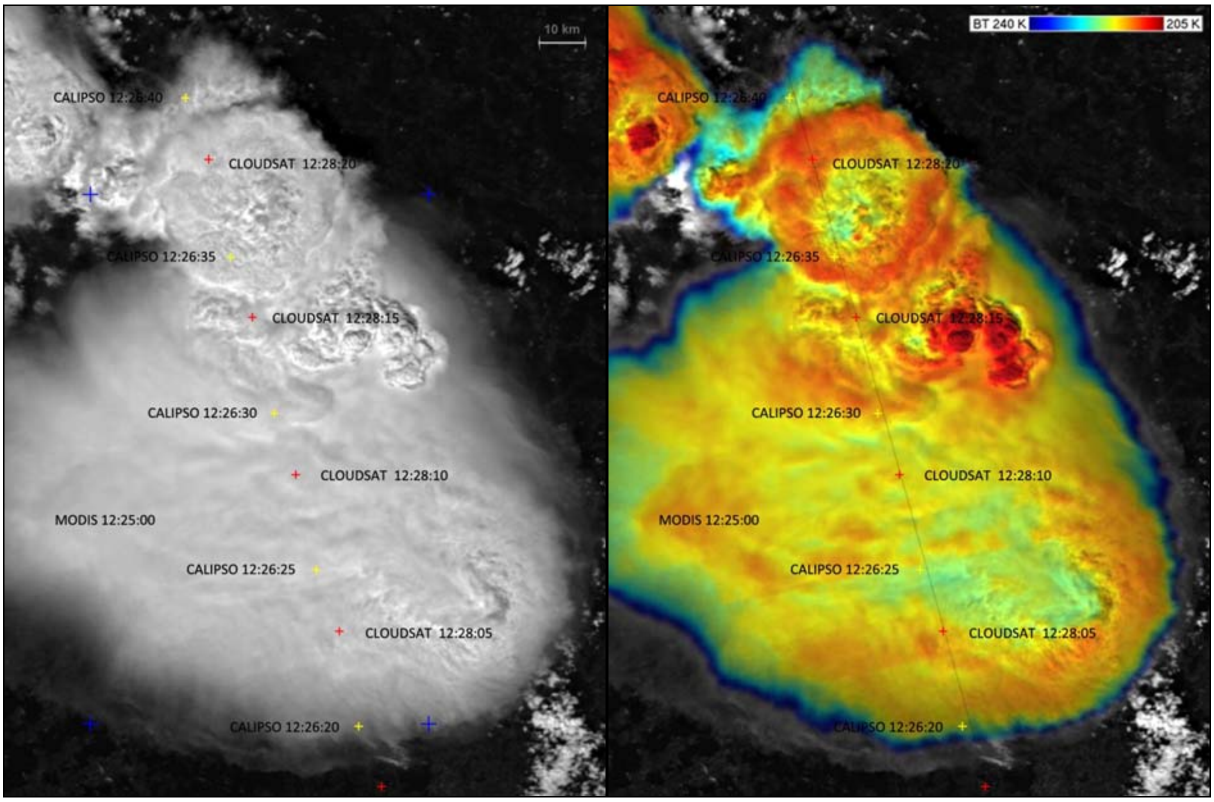

Figure 5: **2013/06/20, 12:25 UTC, MODIS/Aqua. Convective storms above Germany. Left: the 250m band 1 (0.6 µm) image. Crosses indicate ground locations of CloudSat/CPR (red) and CALIPSO/CALIOP (yellow) scan tracks at 5-sec intervals, based on LAT/LON information from HDF data, without a parallax correction. Blue crosses mark LAT/LON grid for better orientation (in the extent of 9-10°E, 50-51°N). Right: sandwich product of band 1 and band 31 (11 µm) with colour enhanced brightness temperature (red - 205 K, blue - 240 K). The line marks out a scan track of CALIOP as determined from the WFC image.**

20. 6. 2013 Germany

The storms over Germany were observed by MSG 2.5-min Rapid Scan, detailed image loops and more information can be found on the web site of the Convection Working Group (Setvák, 2013). Most of the storms which formed on this day were accompanied by severe weather, namely in Switzerland, Germany and the Czech Republic. The storms over central Germany were intersected by A-train satellites (Figure 5 and 6) and according to the ESWD reports (European Severe Weather Database, <essl.org/cgi-bin/eswd/eswd.cgi>) these storms produced large hail up to 6 cm in diameter.

Comparing the MODIS appearance of the storm with the cloud-top trajectory of the CPR and CALIOP profiles (shown in Figure 5) indicates that both of these instruments scanned among others also the area of the cold-ring feature. Tracks of CloudSat and CALIPSO satellites are marked in the MODIS image from 12:25 UTC. The cold-ring feature was observed by CPR in time range from 12:28:16 to 12:28:22 UTC and by CALIOP from 12:26:33 to 12:26:40 (Figure 5 and 6). A part of the warm area inside the cold ring was intersected by these instruments at 12:28:18 (CPR) and 12:26:36 (CALIOP), with no obvious differences in cloud top height between the cold ring and warm area being observed in the two profiles.

The most obvious difference between profiles (shown left in Figure 6) can be found at cloud top level in the centre of the profile (around 12:26:30 in the CALIOP measurement). This feature is composed of smaller ice particles invisible to CPR. Looking at the WFC image, this can be related to a feature which resembles a plume, with its source more to the east (the centre of Figure 5 and Figure 6, right).

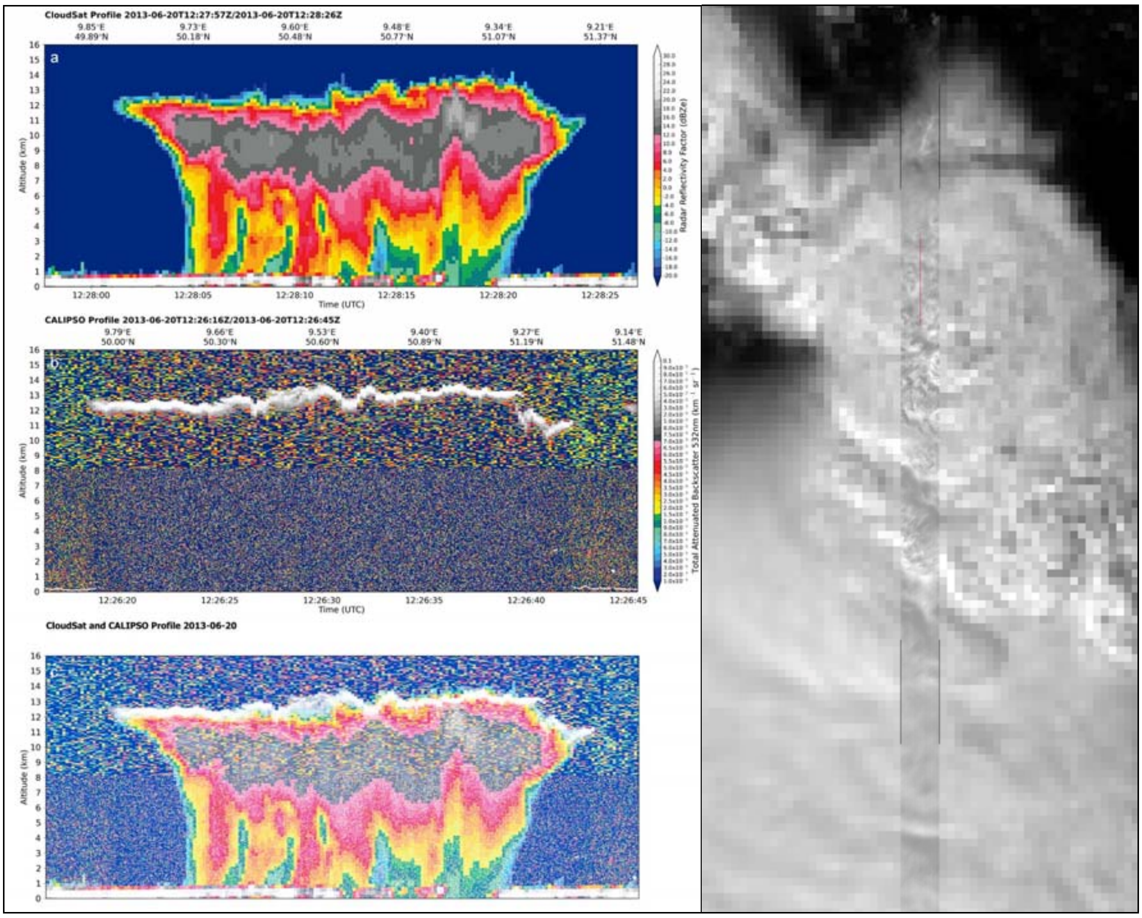

Figure 6: **2013/06/20 Profiles of the storm over Germany and the WFC image, the legend see above in Figure 4.**

DISCUSSION AND FUTURE WORK

Satellite observations of tops of convective storms reveal a number of characteristics that still need to be fully explained in order to enhance our understanding of the processes taking place inside the storms. This brief study focuses on the high-resolution details of distinct OTs (their overall structure, morphology based on high-resolution VIS and near-IR bands, their BT structure and cloud-top microphysics), and their relationship with other cloud-top phenomena. Events of strong convective storms discussed in this study illustrate characteristics and properties of OTs in different perspectives.

Storms exhibiting complex cloud-top structures were almost simultaneously documented by several instruments on polar orbiting satellites, as well as by the Meteosat Rapid Scan. CloudSat and CALIPSO measurements offer an opportunity to study the properties of convective clouds and give a new dimension to our understanding of the overshooting convection. They help to improve our conceptual models of tops of convective storms. Detailed analysis of selected cases clearly showed that for an interpretation of the cloud top phenomena profiles from radar and lidar instruments are very useful. Based on the analysis of these cases it can be said that this study confirms the more recent knowledge of storm-tops and calls for better understanding of their life cycle.

With respect to CPR and CALIOP measurements it should be considered, that the size and the shape of the OT is influenced not only by physics of the process, but also by the phase of development of the OT in time of the observation as well as the position of the cross-sections of the top of the OT. Furthermore, due to the high dynamics of convective processes, the time difference between the crossings of satellites in a formation must be taken into account, especially their interval from the Aqua satellite. In our future work we plan to carry on the storm-top studies among other with the EarthCARE satellite, with its cloud radar and lidar delivering vertical profiles underneath the satellite flight track combined with a multi-spectral imager (www.esa.int/esaLP/Lpearthcare.html). Thus we will not need to deal with the time interval between measurements of the individual instruments as all of these will be aboard one single satellite.

ACKNOWLEDGEMENTS

The authors wish to acknowledge NASA (The Suomi National Polar-orbiting Partnership, CloudSat project, Aqua Project Science and Langley Research Center Atmospheric Science Data Center) and EUMETSAT for their data used in this study. MODIS and NPP images were processed by Martin Setvák; data from CloudSat and CALIPSO were visualized using the program CCPLOT written by Peter Kuma and the WFC images were prepared by Zdeněk Charvát and Martin Setvák. We wish to thank Alois Sokol for his help and technical support. Parts of this work were carried out under the support of the Grant Agency of the Charles University, Prague, Czech Republic, project no. 604812.

REFERENCES

Adler, R. F., Mack R. A. (1986): Thunderstorm Cloud Top Dynamics as Inferred from Satellite Observations and a Cloud Top Parcel Model. *J. of the Atmos. Sciences*, **43**, no. 18, pp 1945-1960

Adler, R. F., Markus, M. J., D. D. (1985): Detection of severe Midwest thunderstorms using geosynchronous satellite data. *Monthly Weather Review*, **113**, pp 769-781

Bedka, K. M., Brunner, J., Dworak, R., Feltz, W., Otkin, J., et al. (2010) Objective satellite-based overshooting top detection using infrared window channel brightness temperature gradients. *Journal of Applied Meteorology and Climatology,* **49**, pp 181–202

Bedka, K. M. (2011) Overshooting cloud top detections using MSG SEVIRI Infrared brightness temperatures and their relationship to severe weather over Europe. *Atmos. Research*, **99**, pp 175-189

Brunner, J. C., Ackerman, S. A., Bachmeier, A. S., Rabin, R. M. (2007): A Quantitative Analysis of the Enhanced-V Feature in Relation to Severe Weather. *Weather and Forecasting*, **22**, pp 853-872

Dworak, R., Bedka, K. M., Brunner, J., Feltz, W. (2012) Comparison between GOES-12 Overshooting-Top Detections, WSR-88D Radar Reflectivity, and Severe Storm Reports. *Weather Forecasting*, **27**, pp 684-699

Kuma, P. (2010) Visualising Data from CloudSat and CALIPSO Satellites. Diploma Thesis, Comenius University, Bratislava, Slovakia, pp 1-79, further information on http://ccplotl.org, June 2013

Levizzani, V., Setvák M. (1996): Multispectral, High-Resolution Satellite Observations of Plumes on Top of Convective Storms, *Journal of the Atmospheric Sciences*, **53**, no. 3, pp 361- 369

Liljas, E. (1984) Processed satellite imageries for operational forecasting. Swedish Meteorological and Hydrological Institute, Norrköping, Sweden, pp 43

Luo, Z., Liu, G. Y., Stephens, G. L. (2008) CloudSat adding new insight into tropical penetrating convection. Geophysical Research Letters, **35**, L19819

McCann, D. W. (1983): The Enhanced-V: A Satellite Observable Severe Storm Signature, *Monthly Weather Review*, **111**, pp 887-894

Rosenfeld, D., Woodley, W. L., Krauss, T. W., Makitov, V. (2006) Aircraft Microphysical Documentation from Cloud Base to Anvils of Hailstorm Feeder Clouds in Argentina. *J. of Applied Met. and Clim.*, **45**, pp 1261-1281

Scorer, R. S. (1986): Cloud Investigation by Satellite. Ellis Horwood Ltd., pp 314

Setvák, M., Bedka, K., Lindsey, D. T., Sokol, A., Charvát, Z., Šťástka, J., Wang, P. K. (2013) A-Train observations of deep convective storm tops. *Atmospheric Research,* **123**, pp 229-248

Setvák, M., Doswelll III, C. A. (1991): The AVHRR channel 3 cloud top reflectivity of convective storms. *Monthly Weather Review*, **119**, pp 842-847

Setvák, M., Charvát, Z., Valachová, M., Bedka, K. (2012): Blended “sandwich“ image products in nowcasting, *Proc. 2012 EUMETSAT Meteorological Satellite Conference*, Sopot, Poland, pp 61

Setvák, M., Levizzani, V. (1992): Influences of NOAA and Meteosat Spatial Resolution on Cloud Top Observations of Deep Convective Storms. *Proc. 9th Meteosat Scientific Users' Meeting*, Locarno, pp 169-174.

Setvák, M. (2013): Focus on the most interesting data of the 2.5-minute rapid scan experiments with MSG satellites. <http://essl.org/cwg/?p=417>, October 2013

Wang, P. K. (2007): The thermodynamic structure atop a penetrating convective thunderstorm. *Atmospheric Research,* **83**, pp 254-262